Microstructure evolution during BaTiO$_3$ formation by solid-state reactions on rutile single crystal surfaces

Andreas Graff, Stephan Senz, Dieter Völtzke*, Hans-Peter Abicht*, and Dietrich Hesse

Max-Planck-Institut für Mikrostrukturphysik, Weinberg 2, D-06120 Halle, Germany

* Institut für Anorganische Chemie, Martin-Luther-Universität Halle-Wittenberg,

Kurt-Mothes-Str. 2, D-06120 Halle, Germany

1

Abstract:

During sintering of TiO_2-$BaCO_3$ core-shell powders a modified phase formation sequence had been observed compared to the common powder sintering process. To study this phenomenon model experiments concerning phase formation and microstructure evolution during $BaTiO_3$ genesis were performed. Reaction products between BaO vapour and TiO_2 (rutile) single crystals with different orientations, obtained at different temperatures, were investigated by XRD texture analysis, high resolution TEM (HRTEM) and electron energy loss spectroscopy (EELS).

At a substrate temperature of 700°C nanocrystalline $BaTiO_3$ grows as a reaction product. $BaTiO_3$ was also found in reactions performed at 800°C and 850°C with Pt markers on the initial TiO_2 surface. In-diffusion of Ba ions can explain the position of the Pt particles above the $BaTiO_3$ phase after the reaction. Crystallites of Ti-rich phases were found between the $BaTiO_3$ layer and the TiO_2 substrate after reactions at 850°C. At 900°C, $BaTiO_3$ forms at the surface of the reaction layer. It has a well-defined orientation relation to the rutile substrate. In addition to $BaTiO_3$, Ti-rich phases and pores were identified at the $BaTiO_3$-TiO_2 interface. Ti-rich phases most probably form by a reaction between the substrate and the initially grown $BaTiO_3$ thin reaction layer. The pore formation is explained by an out-diffusion of titanium and oxygen ions from the $BaTiO_3$-TiO_2 interface through the reaction layer to the surface.

1. Introduction

BaTiO$_3$ ceramics are widely used because of their favourable dielectric and ferroelectric properties. To improve the microstructure of BaTiO$_3$ ceramics, attempts have been made to structurally modify the precursors [1]. Core-shell powders show a modified phase evolution during the sintering process [2]. In addition to the Ba-rich orthotitanate Ba$_2$TiO$_4$, Ti-rich phases can be observed depending on the annealing temperature. The local appearance of the different phases was determined by Raman microscopy [3]. This complex reaction mechanism should be accessible more easily in model experiments. In experiments with planar polycrystalline substrates, BaTiO$_3$ was found to be the first reaction product, forming by in-diffusion of Ba and O ions into the TiO$_2$ lattice [4]. In a previous work we determined the formation of Ti-rich phases in the system SiO$_2$-BaTiO$_3$ using BaTiO$_3$ single crystals [5]. During growth of BaTiO$_3$ on TiO$_2$ single crystals in a barium flux, topotaxial reactions take place at the reaction front leading to a well-defined orientation relation between TiO$_2$ and BaTiO$_3$ [6]. In this paper the orientation and the sequence of reaction products during reactions between BaO vapour and TiO$_2$ (rutile) single crystals is studied, and the consequences in terms of the reaction mechanism are discussed.

2. Experimental

As substrates 10x10x1 mm^3 rutile single crystal substrates of four different orientations (100), (001), (110), and (101) were used. Before the experiments the substrates were annealed in air up to 900°C for 10 min. For the reaction experiments between Ba-oxide vapour and the rutile single crystals, BaCO$_3$ targets were evaporated in a high vacuum chamber by electron beam evaporation, and the heated rutile crystals were exposed to the generated vapour beam. The oxygen background pressure was 1x10^{-2} Pa raising to 1x10^{-1} Pa during the experiment. The deposition rate was 0.1 nm/sec. The substrates were heated to either 700°C, 800°C, 850°C, or

900°C in a tube furnace. After the experiment the substrates were allowed to cool down with a rate of ~ 10 K per minute. For marker experiments a thin film of platinum was deposited by magnetron sputtering followed by an annealing to 1000°C to form small Pt-spheres on the rutile surface. The formation of the Pt-particles was evaluated by atomic force microscopy (AFM).

The phases formed were first characterized by X-ray diffraction (XRD). Θ-2Θ measurements were performed to identify the oriented and polycrystalline reaction products. To evaluate the orientation of the grown phases pole figure measurements were performed for certain 2Θ angles. Cross section samples for transmission electron microscopy (TEM) were prepared by conventional techniques including sawing, polishing, dimpling and ion milling. The cross sections were investigated by conventional TEM, high resolution TEM (HRTEM; Jeol 4010 EX), and electron energy loss spectroscopy (EELS; Philips CM 20 FEG with Gatan Imaging Filter).

3. Results

At a reaction temperature of 700°C, $BaTiO_3$ is formed as a reaction product in the solid-vapour reaction. The orientation of the $BaTiO_3$ layer partly depends on the orientation of the rutile substrate surface. For the (100) and (110) rutile orientations most of the $BaTiO_3$ films grow with a well-defined orientation to the substrate. Θ-2Θ XRD measurements show the appearance of the characteristic reflections of $BaTiO_3$ beside the substrate reflections. In Figs. 1a,b texture measurements reveal the different orientations of the $BaTiO_3$ lattice planes parallel to the surface of the (100) and (110) rutile substrates, respectively. In the case of the (100) substrate, (112) $BaTiO_3$ $\parallel$ (100) Rutile. In the case of the (110) rutile substrate most of the $BaTiO_3$ regions have their (100) planes parallel to the (110) rutile surface. In both cases the XRD results correspond to the TEM investigations. The cross-section micrographs in Fig-

ure 2 show the reaction layer on top of the rutile (100) substrate. A roughening of the (100) surface occurs. Looking along the [001] rutile direction (Fig. 2a), (110) facets of the rutile are visible. On these facets, $BaTiO_3$ crystallites are formed as shown by HRTEM (Fig. 2b). Interestingly the faceting of the surface is caused by the reaction, which was counterchecked by AFM of a substrate simply heated in high vacuum at 800°C revealing the surface staying flat. On (110) rutile substrates the reaction layer consists of small grains. The interface to the rutile is less rough and not faceted (Fig. 3). The orientation relation found by HRTEM is:

$BaTiO_3$ (001) || Rutile (110); $BaTiO_3$ [1$\bar{1}$0] || Rutile [1$\bar{1}$0]
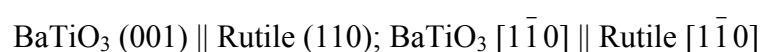
This orientation relation is in agreement with the one deduced from XRD measurements. (Note: For convenience, for the HRTEM investigations the lattice of $BaTiO_3$ is regarded as cubic with a lattice parameter $a = 0.4$ nm.)

Experiments at 800°C and 850°C were performed on rutile substrates with Pt particles on the surface. These particles should act as inert markers for the initial interface. This requires the immobility of the Pt islands during the reaction. Pt particles of diameters of some tens of nanometer (determined by AFM) were used.

XRD measurements of the samples prepared at 800°C (not shown) indicate the formation of $BaTiO_3$ as a reaction product. Pole figures indicate the presence of an oriented part of $BaTiO_3$ on all rutile substrates. TEM cross sections of these films show, however, the generally polycrystalline structure of the deposited and reacted film. Figure 4 demonstrates the situation for the (001) rutile substrate. The interface between the substrate and the reaction products is rough. The surface of the reaction layer is not flat either. These results indicate a reaction mechanism, which incorporates diffusion parallel to the interface. The Pt particles can be found on top of the crystalline reaction products (Fig. 4a). HRTEM investigations of the lattice fringes reveal $BaTiO_3$ as the reaction product. The position of the Pt islands on top of the reaction product might result from in-diffusion of Ba ions, but could also occur because the

oxides are not sufficiently wetting the noble metal. For the (001) and (110) rutile surfaces, respectively, the orientation relations are:

(110) $BaTiO_3$ ∥ (001) Rutile; [001] $BaTiO_3$ ∥ [1$\bar{1}$0] Rutile

(001) $BaTiO_3$ ∥ (110) Rutile; [1$\bar{1}$0] $BaTiO_3$ ∥ [1$\bar{1}$0] Rutile

Some amorphous layer can be found on top of the $BaTiO_3$ film, most probably due to unreacted BaO or $BaCO_3$.

Marker experiments at 850°C show the appearance of an additional Ba-Ti-O phase. The reaction layer consists of grains (Fig. 5). In the HRTEM image (Fig. 5b) the formation of an additional phase can be recognised between the rutile substrate and the $BaTiO_3$ film. Stacking faults as the ones visible in Figure 5b are typical for Ti-rich phases grown by solid state reactions [7]. The Ti-rich phase $Ba_4Ti_{13}O_{30}$ was identified by the fast Fourier transform (FFT; Fig. 5d) of the HRTEM image (Fig. 5c). The (001) interplanar distance of $Ba_4Ti_{13}O_{30}$ is about 1.4 nm which is roughly six times the interplanar distance of (111) $BaTiO_3$. Indeed these two lattice planes are parallel to each other: $BaTiO_3$ (111) ∥ $Ba_4Ti_{13}O_{30}$ (001), indicating a topotaxial formation mechanism.

Experiments at 900°C without marker show the presence of different Ti-rich phases at the interface with the rutile substrate, identified by their large lattice constant (Fig. 6). In addition holes are formed at this interface. On top of the Ti-rich grains some $BaTiO_3$ remains with a well defined orientation to the rutile substrate. EELS measurements prove the formation of the Ti-rich phases at the interface with the rutile substrate as demonstrated in the line scan of Figure 7. The evaluation of the spectra of grain 2 results in a molar Ba-to-Ti ratio of about 1 to 2 for the Ti-rich phase.

4. Conclusions

BaTiO$_3$ forms as the first product in the reaction between BaO vapour and rutile single crystals. In spite of differently oriented rutile substrates used, most of the identified orientation relationships of the BaTiO$_3$ phase involve the relation (001) BaTiO$_3$ ‖ (110) Rutile. This is probably due to the small lattice mismatch (~ 4%). Marker experiments show that the first BaTiO$_3$ grains form by in-diffusion of Ba ions into the TiO$_2$. Experiments at higher temperatures show the growth of well-oriented Ti-rich Ba-Ti-O phases, which form by out-diffusion of Ti ions from the substrate into the initially grown BaTiO$_3$ layer. The pore formation at 900°C can also be explained by the out-diffusion of Ti and oxygen ions from the rutile crystal. The results demonstrate that in the BaO-TiO$_2$ system diffusing species, phase formation sequence, and morphology and orientation of the product phases are a complex function of the reaction conditions. Further work is required before more definite conclusions can be drawn, in particular concerning phase formation in core-shell powders.

References

1. Gablenz, S., Damm, C., Müller, F., Israel, G., Rössel, M., Rössel, M., Röder, A., Abicht, H.-P., Preparation and characterization of core-shell structured TiO$_2$–BaCO$_3$ particle. *Solid State Sci.*, 2001, **3**, 291-299.

2. Rössel, M., Gablenz, S., Müller, T., Röder, A., Abicht, H.-P., A core-shell structured BaTiO$_3$ precursor preparation, characterization and potential. *Anal. Bioanal. Chem*, 2003, **375**, 310-314.

3. Rössel, M., Höche, H.-R., Leipner, H. S., Völtzke, D., Abicht, H.-P., Hollrichter, O., Müller, J., Gablenz, S., Raman microscopic investigations of $BaTiO_3$ precursors with core-shell structure. *Anal. Bioanal. Chem*, 2004, submitted.

4. Beauger, A., Mutin, J. C., Niepce, J. C., Synthesis reaction of metatitanate $BaTiO_3$. *J. Mater. Sci.*, 1983, **18**, 3543-3550.

5. Senz, S., Graff, A., Blum, W., and Hesse, D., Orientation relationsships of reactievely grown $Ba_2TiSi_2O_8$ on $BaTiO_3$ (001) determined by X-ray diffractometry. *J. Am. Ceram. Soc.*, 1998, **81**, 1317-1321.

6. Suyama, Y., Oda, Y., and Kato, A.,Topotaxy between TiO_2 and $BaTiO_3$. *Chemistry Letters*, 1979, **8,** 987-988.

7. Hesse, D., Graff, A., Senz, S., and Zakharov, N. D., Topotoxial reaction fronts in complex Ba-Ti-Si oxide systems studied by transmission electron microscopy. *Mater. Sci. Forum*, 1999, **294-296**, 597-600.

Figure Captions

Figure 1: XRD pole figures (Center: $\psi = 0°$; rim: $\psi = 90°$) measured at $2\Theta = 31,37°$ for the BaTiO$_3$ (110) planes after the BaO-TiO$_2$ vapour-solid reaction at 700°C (a) on (100), and (b) on (110) rutile substrates. An oriented growth of BaTiO$_3$ is observed on both substrates.

Figure 2: TEM cross section micrographs of samples after reaction of a BaO vapour with a (100) rutile substrate at 700 °C. a) Formation of (110) rutile facets underneath the reaction layer; b) Lattice plane image of the reaction product BaTiO$_3$; c) Corresponding image of the substrate in the [001] viewing direction.

Figure 3: TEM cross section micrographs of the reaction layer on a rutile (110) surface grown at 700°C. a) Overview; b) Magnified image of a BaTiO$_3$ grain; c) and d) Computer-processed lattice plane images of reaction layer and substrate, respectively.

Figure 4: TEM cross section micrographs of a reaction experiment performed at 800°C on rutile (001). Viewing direction is [001] BaTiO$_3$ || [1$\bar{1}$0] Rutile. a) Overview; b) and c) Processed lattice plane images of the rutile substrate and a BaTiO$_3$ grain, respectively.

Figure 5: TEM cross section micrographs of reaction products formed at 850°C on the rutile (100) surface; a) Overview; b) Formation of a Ti-rich phase between the substrate and the BaTiO$_3$ layer; c) Processed lattice plane image of the interface between the Ti-rich phase and the BaTiO$_3$ layer; d) FFT of image (c); the BaTiO$_3$ reflections are connected by the grid.

Figure 6: Cross section of a reaction layer grown at 900°C on the (100) rutile surface. a) Large holes are formed at the interface between the substrate and the reaction layer. b) $BaTiO_3$ can be found on top of the Ti-rich phase. c)-e) Lattice plane images of reaction products and the substrate (magnified sections of image (b)).
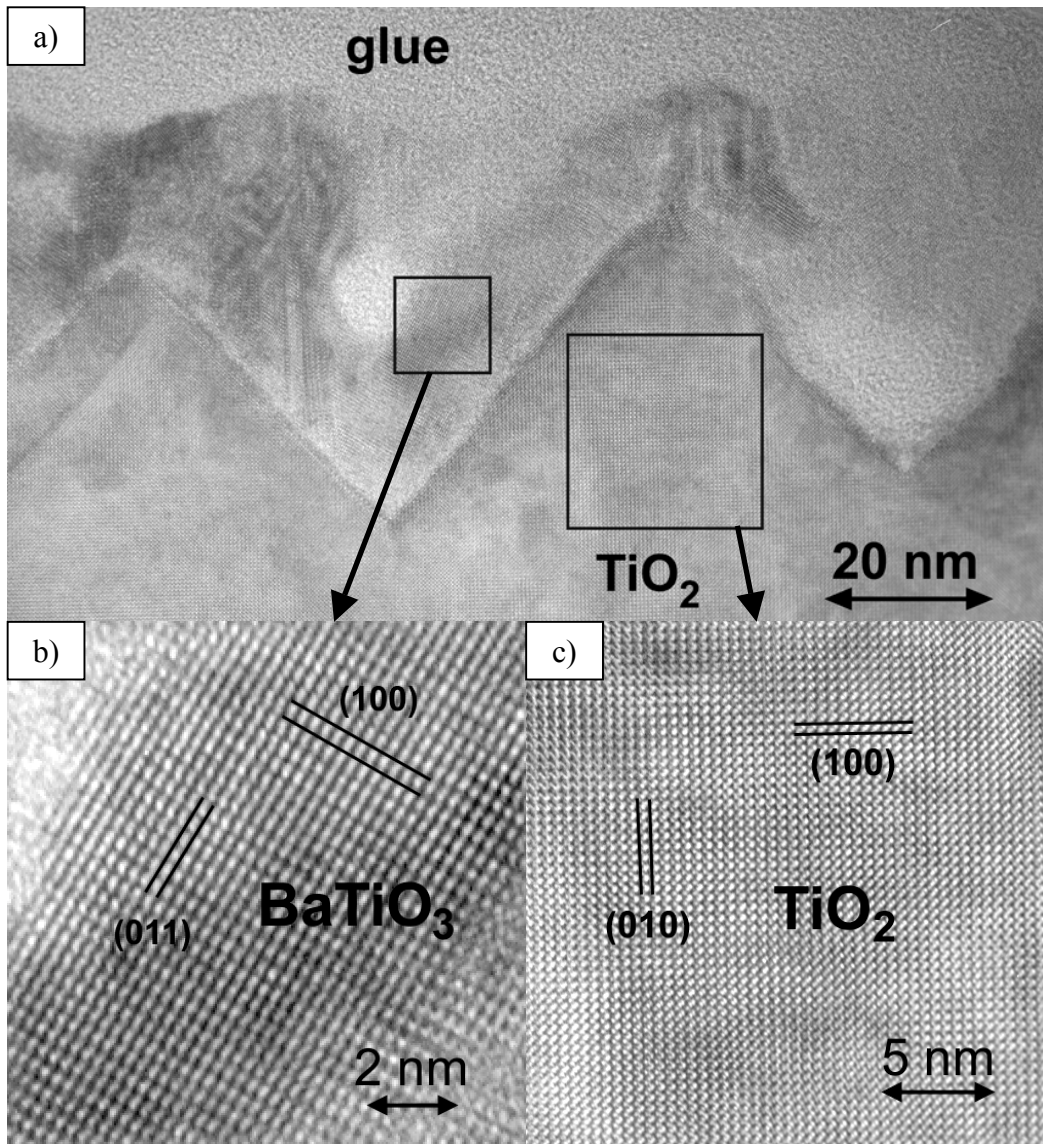
Figure 7: a) TEM cross section micrograph of the reaction layer on a rutile (101) substrate. The line indicates the track of the EELS line scan from surface to substrate; b) EELS spectra; c) EELS spectra of grain 1, 2 and substrate, respectively.
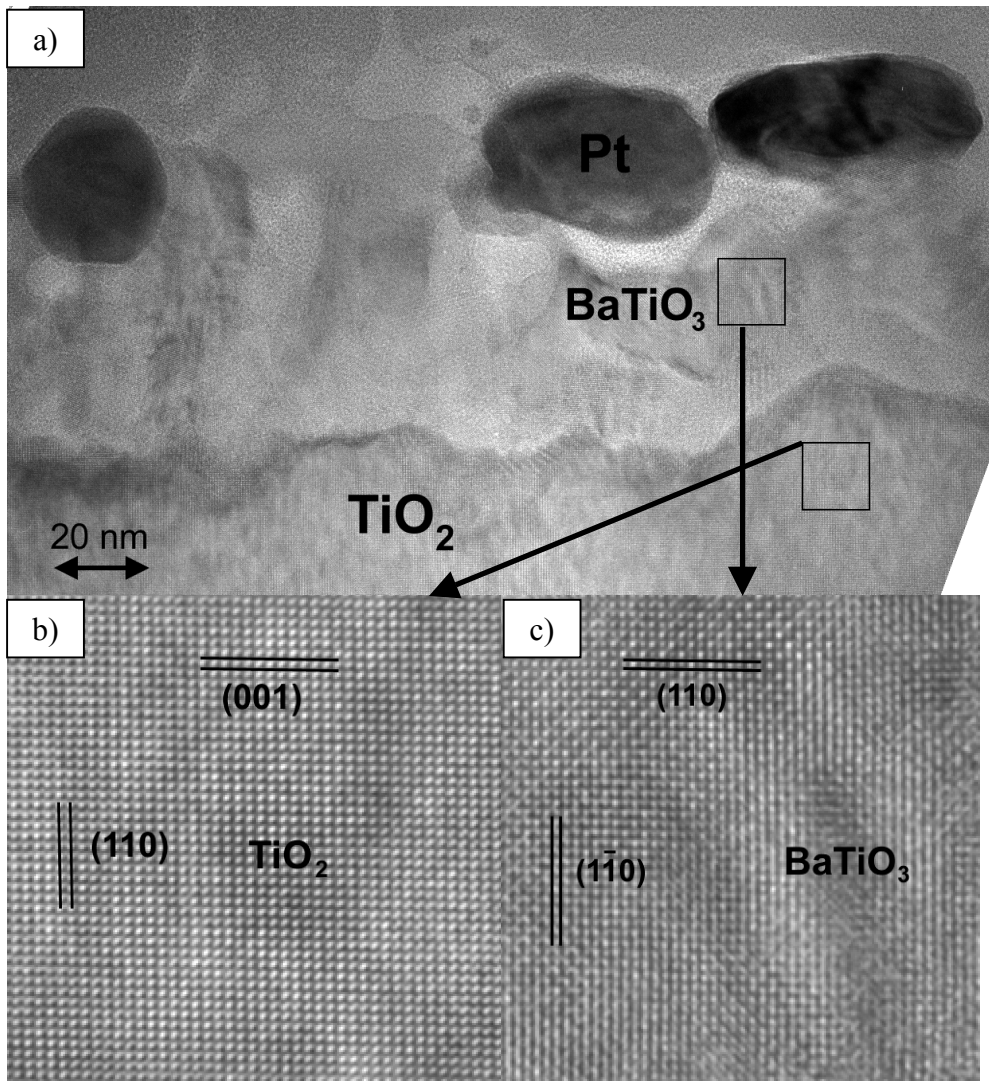
Figure 1

a)
b)
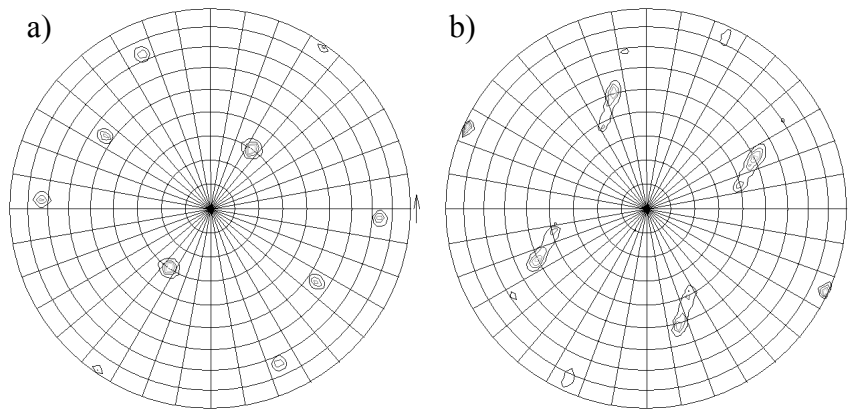
A. Graff *et. al.*

Figure 2

A. Graff *et. al.*

Figure 3

A. Graff *et. al*

Figure 4

a)

Pt

BaTiO$_3$

TiO$_2$

20 nm

b)

(001)

(110) TiO$_2$

c)

(110)

(1$\bar{1}$0) BaTiO$_3$
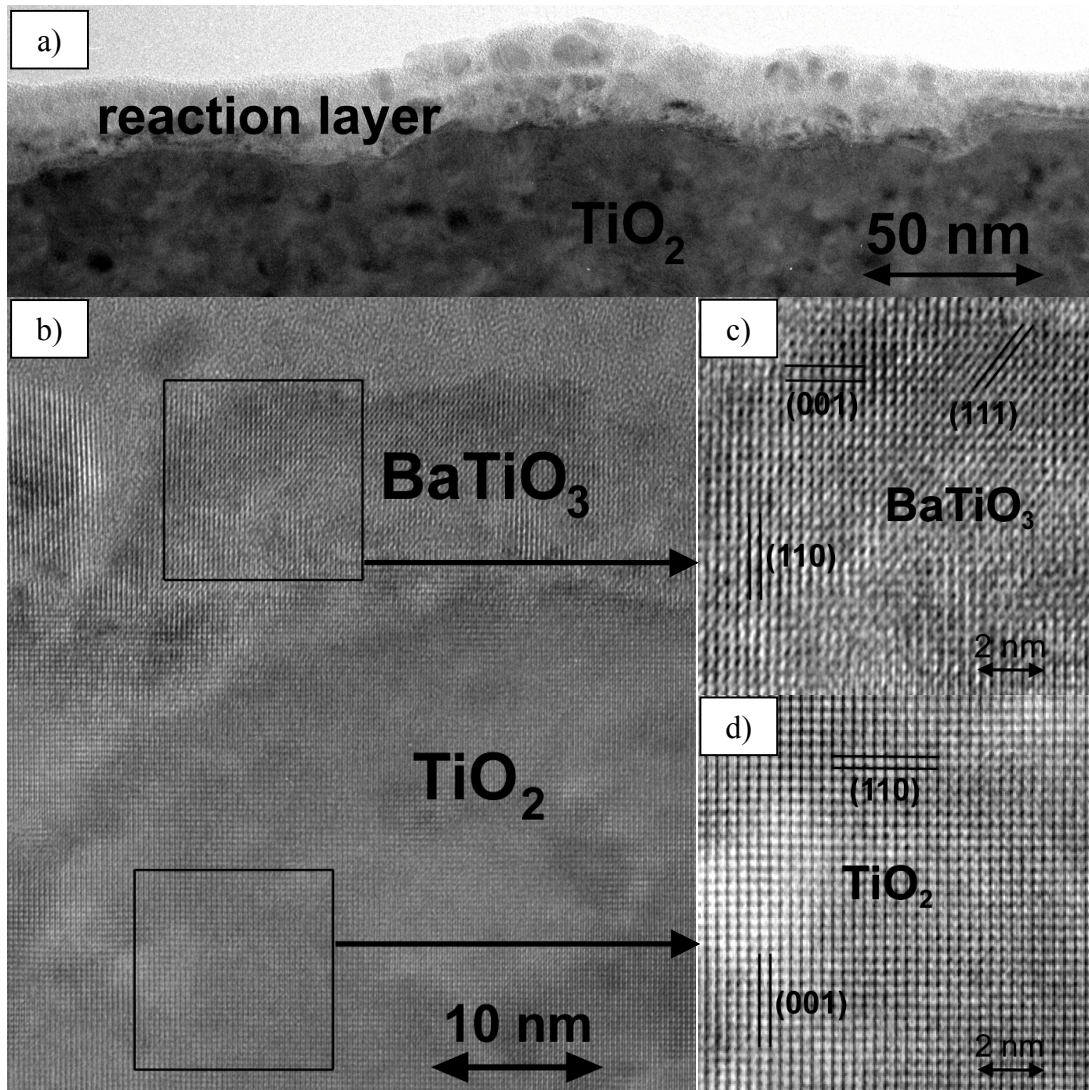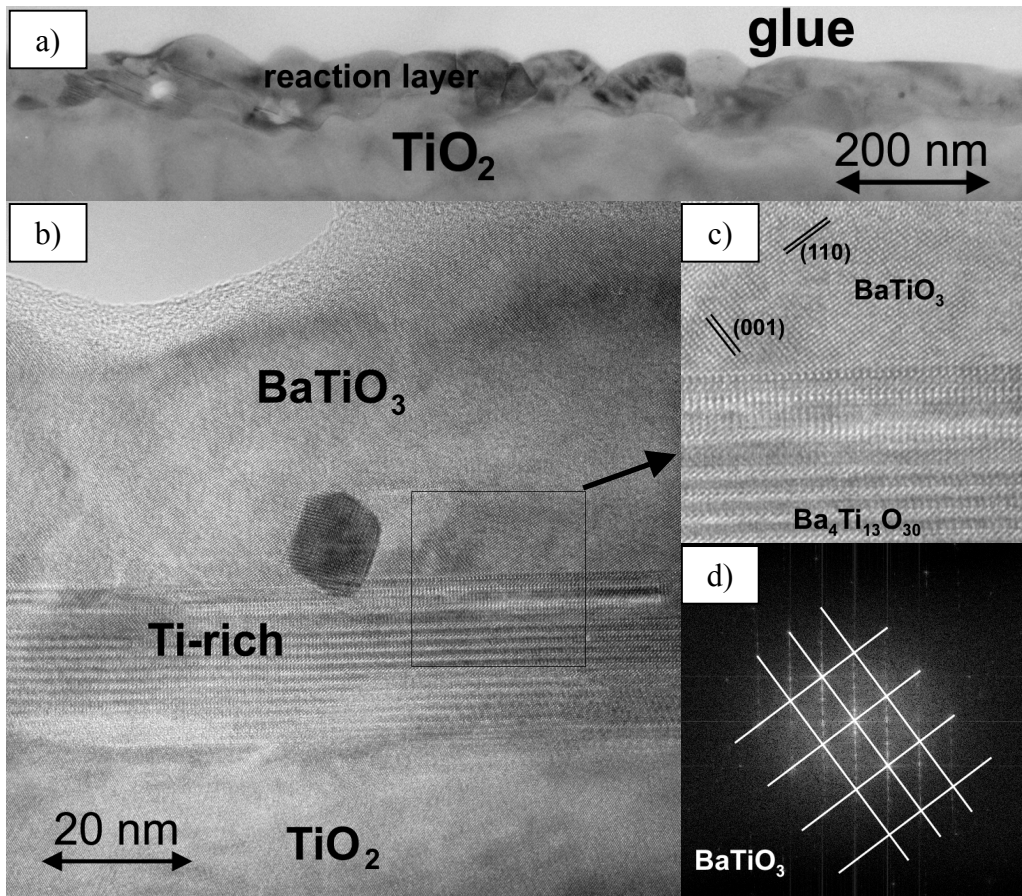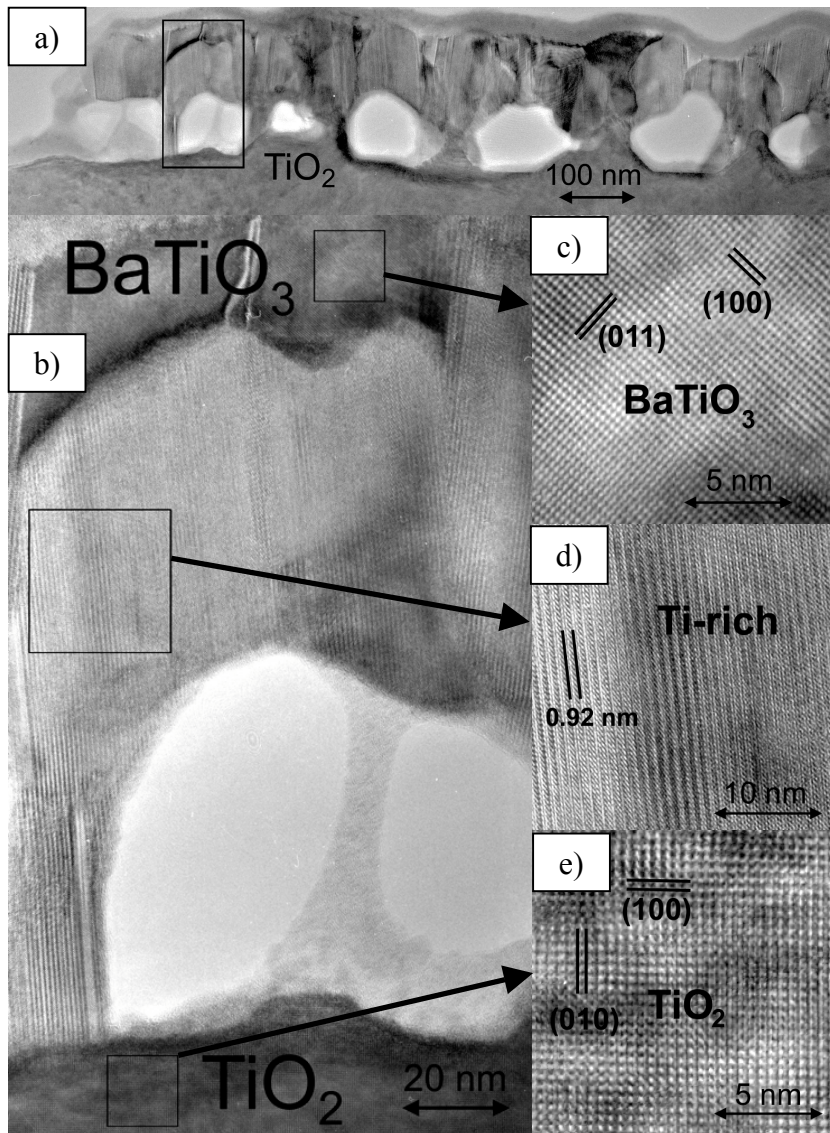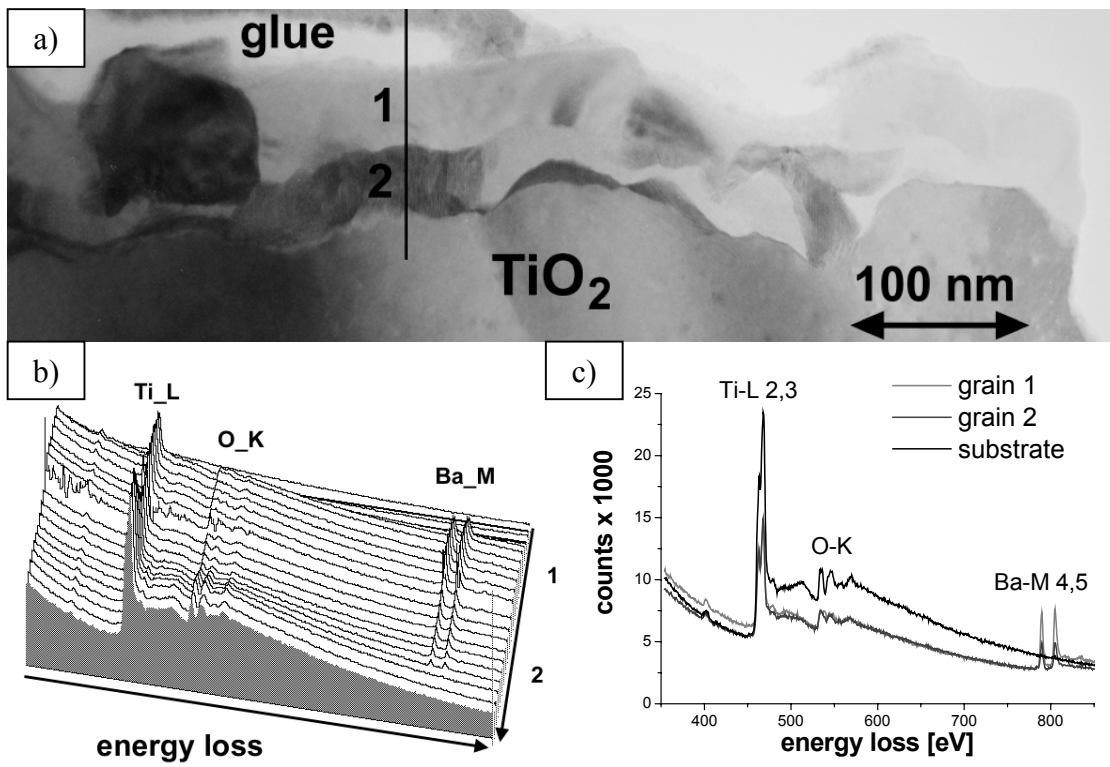
A. Graff *et. al*

Figure 5

A. Graff *et. al*

Figure 6

A. Graff *et. al*

Figure 7

A. Graff *et. al*